2015

Theory of bimolecular reactions in a solution with linear traps: application to the problem of target search on DNA

Alexander Turkin
University of Groningen

Antoine M. van Oijen
University of Groningen, vanoijen@uow.edu.au

Anatoliy Turkin
National Science Center Kharkov Institute of Physics and Technology

Publication Details

Turkin, A., van Oijen, A. M. & Turkin, A. (2015). Theory of bimolecular reactions in a solution with linear traps: application to the problem of target search on DNA. Physical Review E: Statistical, Nonlinear, and Soft Matter Physics, 92 (5), 52703-1 - 52703-14.

Theory of bimolecular reactions in a solution with linear traps: application to the problem of target search on DNA

Abstract

One-dimensional sliding along DNA as a means to accelerate protein target search is a well-known phenomenon occurring in various biological systems. Using a biomimetic approach, we have recently demonstrated the practical use of DNA-sliding peptides to speed up bimolecular reactions more than an order of magnitude by allowing the reactants to associate not only in the solution by three-dimensional (3D) diffusion, but also on DNA via one-dimensional (1D) diffusion [A. Turkin et al., Chem. Sci. (2015)]. Here we present a mean-field kinetic model of a bimolecular reaction in a solution with linear extended sinks (e.g., DNA) that can intermittently trap molecules present in a solution. The model consists of chemical rate equations for mean concentrations of reacting species. Our model demonstrates that addition of linear traps to the solution can significantly accelerate reactant association. We show that at optimum concentrations of linear traps the 1D reaction pathway dominates in the kinetics of the bimolecular reaction; i.e., these 1D traps function as an assembly line of the reaction product. Moreover, we show that the association reaction on linear sinks between trapped reactants exhibits a nonclassical third-order behavior. Predictions of the model agree well with our experimental observations. Our model provides a general description of bimolecular reactions that are controlled by a combined 3D+1D mechanism and can be used to quantitatively describe both naturally occurring as well as biomimetic biochemical systems that reduce the dimensionality of search.

Disciplines

Medicine and Health Sciences | Social and Behavioral Sciences

Publication Details

Turkin, A., van Oijen, A. M. & Turkin, A. (2015). Theory of bimolecular reactions in a solution with linear traps: application to the problem of target search on DNA. Physical Review E: Statistical, Nonlinear, and Soft Matter Physics, 92 (5), 52703-1 - 52703-14.

Theory of bimolecular reactions in a solution with linear traps: Application to the problem of target search on DNA

Alexander Turkin,[1,*] Antoine M. van Oijen,[1,†] and Anatoliy A. Turkin[2]

[1]*Single-Molecule Biophysics, Zernike Institute for Advanced Materials, University of Groningen, Nijenborgh 4, Groningen 9747 AG, Netherlands*

[2]*National Science Center "Kharkiv Institute of Physics & Technology," Akademichna street 1, Kharkiv 61108, Ukraine*

(Received 26 May 2015; revised manuscript received 18 September 2015; published 3 November 2015)

One-dimensional sliding along DNA as a means to accelerate protein target search is a well-known phenomenon occurring in various biological systems. Using a biomimetic approach, we have recently demonstrated the practical use of DNA-sliding peptides to speed up bimolecular reactions more than an order of magnitude by allowing the reactants to associate not only in the solution by three-dimensional (3D) diffusion, but also on DNA via one-dimensional (1D) diffusion [A. Turkin *et al.*, Chem. Sci. (2015)]. Here we present a mean-field kinetic model of a bimolecular reaction in a solution with linear extended sinks (e.g., DNA) that can intermittently trap molecules present in a solution. The model consists of chemical rate equations for mean concentrations of reacting species. Our model demonstrates that addition of linear traps to the solution can significantly accelerate reactant association. We show that at optimum concentrations of linear traps the 1D reaction pathway dominates in the kinetics of the bimolecular reaction; i.e., these 1D traps function as an assembly line of the reaction product. Moreover, we show that the association reaction on linear sinks between trapped reactants exhibits a nonclassical third-order behavior. Predictions of the model agree well with our experimental observations. Our model provides a general description of bimolecular reactions that are controlled by a combined 3D+1D mechanism and can be used to quantitatively describe both naturally occurring as well as biomimetic biochemical systems that reduce the dimensionality of search.

DOI: 10.1103/PhysRevE.92.052703 PACS number(s): 82.39.−k, 82.20.−w, 87.15.R−

I. INTRODUCTION

The importance of dimensionality in the diffusive transport of biological molecules has long been recognized. Almost half a century ago, Adam and Delbruck provided theoretical proof that diffusion-based reactions can be significantly accelerated by reducing the dimensionality of search [1]. First experimental evidence of this concept was reported in 1970, when Riggs *et al.* [2] found that the association rate of *lac* repressor to its binding site is two orders of magnitude higher than predicted by association via three-dimensional (3D) diffusion in solution. Subsequent detailed experimental and theoretical studies of this phenomenon by von Hippel, Berg, and colleagues became classical works in the field [3–6]. The authors proposed several possible mechanisms of reaction speedup, including one-dimensional (1D) random walk along DNA, 1D hopping on DNA, 3D jumping, and intersegmental transfer. This model was revisited by Halford and Marko [7], who significantly simplified it by introducing the mean sliding length as a main parameter. A similar result was obtained by Klenin *et al.* [8] starting from first principles. Though not being able to provide direct observation of any of the proposed reaction pathways, ensemble studies significantly advanced our understanding of diffusion-based search and provided much support for facilitated diffusion mechanisms [9,10]. Direct unprecedented observations of protein movement along DNA was made possible by the recently developed single-molecule techniques. Different polymerases, transcription factors, DNA-repair proteins, and virulence factors were shown to slide along DNA in a 1D fashion [10]. The visualization of fluorescently labeled proteins sliding on stretched DNA revived the interest in the topic of diffusion-based target search. Several analytical [8,11–14] and simulation [8,15–19] models were proposed; nowadays it is generally accepted that a combination of 3D and 1D diffusion contributes to target search.

Recently, we attempted to recreate nature's solution to the target search problem and to apply the concept of 1D diffusion to accelerate a biotechnological as well as an artificial model system (Fig. 1). To make our reacting species able to slide along DNA we chose pVIc, a naturally occurring 11-a.a. peptide that is involved in adenovirus maturation. In particular, the peptide helps a small number of proteases find a large number of targets within tightly packed viral particles by allowing protease enzymes to 1D diffuse along the viral DNA. The interior of the viral capsids is so crowded that relying solely on 3D diffusion would make target search impossible. One-dimensional sliding of pVIc along DNA was confirmed *in vitro* using single-molecule microscopy methods [20,21]. In a biomimetic approach, we coupled the sliding peptides to primers in a conventional polymerase chain reaction (PCR) and demonstrated a 15%–27% acceleration of amplicon formation as compared to unfunctionalized primers [22]. Furthermore, to show the generality of our approach we designed a model system with two reactants, which were equipped with the pVIc peptide, and DNA was added to the solution as a catalyst for the reaction.

As reactants we chose biotin and streptavidin. The reaction progress was recorded in real time by detecting the Förster resonance energy transfer (FRET) signal arising from the association of fluorescently labeled reactants. By varying the concentration and the length of the DNA fragments,

*Corresponding author: o.turkin@rug.nl

†Present address: School of Chemistry, University of Wollongong, Wollongong, NSW 2522, Australia.

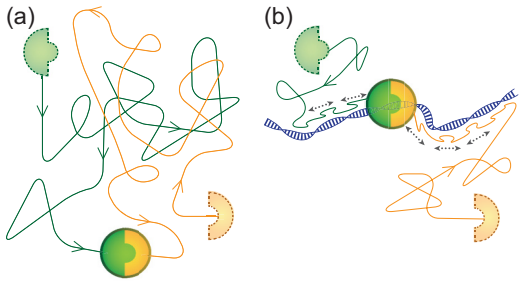

FIG. 1. (Color online) Speeding-up association reactions between biomolecules due to one-dimensional diffusion along DNA. Instead of relying only on 3D diffusion (a), reactants that are functionalized by DNA-sliding peptides are able to find each other faster by means of 1D sliding over DNA, which is present in solution as a catalyst (b).

we changed the reaction rates. In the optimal regime we observed a more than one order of magnitude reaction speedup. We studied the dependence of the reaction time on DNA concentration for DNA fragments of different lengths and concluded that the reaction time depends mainly on the total DNA base pair concentration that is proportional to the product of DNA fragments concentration and their length [22].

In this paper, we formulate a phenomenological model to rationalize our findings in the study of the reaction kinetics between pVIc functionalized biotin and streptavidin in a solution with DNA. The model predicts the time evolution of the reaction product amount for different DNA lengths and concentrations. In contrast to previous models, where a probabilistic approach is used to mainly focus on individual molecular species, our model describes an ensemble-averaged behavior of the bimolecular system with DNA.

In the next section we use the mean-field approach to construct a set of reaction rate equations for the concentrations of two reacting molecular species in a solution with DNA molecules that act as linear traps (sinks). The model takes into account the exchange of molecules between linear traps and solution. Being trapped by a linear sink, a molecule undergoes random walks along the sink; it can meet the reaction partner before detrapping. The model considers three reaction pathways: (i) reaction in the solution controlled by 3D diffusion, (ii) reaction of molecules diffusing from the solution to their partners trapped by linear sinks, and (iii) reaction between molecules trapped by linear sinks, which is controlled by 1D diffusion. In fact the third mechanism is a combination of 3D search of a linear sink and 1D search of a reaction partner trapped on the same linear sink.

In Sec. III the model equations are solved numerically with the parameters appropriate to our experimental system. When evaluating the fitting parameters of the model we discuss the role of electrostatic interaction and orientation constraints for the reaction. The characteristic reaction time obtained from the model is compared to the reaction time observed experimentally for a wide concentration range of DNA segments. We calculate the contribution of each reaction mechanism as a function of linear sink concentration. The important conclusion is that at the optimum concentration of liner sinks the 1D mechanism dominates. In our experimental system it is as high as 90%.

The proposed model provides insights regarding the reaction acceleration by 1D diffusion. This model builds a bridge between protein biophysics and the newly emerging approach of chemistry in reduced dimensionality.

II. MEAN-FIELD MODEL

Facilitated DNA search via 1D diffusion is a manifestation of a general physical mechanism of 1D bimolecular reactions that is discussed in the physical chemical literature [23–29]. In this section we will omit the biology-specific terms and will use a physical language. Let us consider the irreversible reaction between A and B molecules in a buffer solution with DNA fragments. We denote the reaction product as C. Reactants can associate in solution due to 3D random walks as well as on DNA molecules due to 1D random walks. DNA molecules, henceforth called D sinks, act as linear traps that trap molecules A and B. The diffusion mobility of D sinks is assumed to be small as compared to diffusional mobility of A and B molecules, which is valid for long DNA fragments with molecular weights much higher than those of A and B.

Our goal is to construct a model describing the kinetics of the chemical reaction between A and B molecules in the 3D space and on one-dimensional D sinks. In particular, the reaction output—concentration of C molecules $C_C(t)$—has to be found as a function of time and input parameters. To this end we use the mean-field approach or the effective lossy medium that has been developed for description of radiation effects in nuclear materials [30,31].

On a microscopic scale, the molecule A concentration $C_A(\mathbf{r},t)$ changes with time according to a conservation equation that describes Fick's diffusion and the local reaction in the solution,

$$\frac{\partial C_A}{\partial t} = -div\mathbf{j}_A - \alpha_{AB} C_A C_B, \tag{1}$$

with appropriate boundary conditions on all D sinks. Here, and throughout this section, concentrations are defined per unit volume. The corresponding equations for molecules B can be obtained by interchanging the labels A and B. In Eq. (1) the second term on the right-hand side describes the reaction in the bulk. The diffusion flux $\mathbf{j}_A$ is given by a well-known expression,

$$\mathbf{j}_A = -D_A \nabla C_A - \frac{D_A C_A}{k_B T} \nabla W_A, \tag{2}$$

where D_A is the 3D diffusion coefficient of molecules A and W_A is the interaction energy with the microscopic electrostatic potential in the solution. In the diffusion-limited case the reaction rate constant between ions in a solution was derived by Debye [32] following the Smoluchowski method [33],

$$\alpha_{AB} = 4\pi \eta_{AB} (D_A + D_B) \left[\int_{r_0}^{\infty} \exp\left(\frac{U}{k_B T}\right) \frac{dr}{r^2} \right]^{-1}, \tag{3}$$

where $r_0 = r_A + r_B$ is the sum of molecule radii taken as the reaction (or capture) distance, and U is the interaction energy between A and B molecules. The Smoluchowski-Debye result, Eq. (3), is an upper bound to the reaction rate constant. This result was derived for reactant molecules with isotropic reactivity and is unrealistic for stereospecific binding of

TABLE I. Parameters used in numerical calculations.

Parameter	Value	Reference
Temperature, T (K)	293	[22]
Dielectric constant of solution, ε	62	[50]
Solution viscosity, μ (kg m^{-1} s^{-1})	10^{-2}	[22]
Initial concentration of A molecules, C_{A0} (nM)	40	[22]
Initial concentration of B molecules, C_{B0} (nM)	80	[22]
NaCl concentration in the buffer solution, $C_{\rm buf}$ (M)	2×10^{-3}	[22]
Radius of A molecules, r_A (nm)	3	See text
Radius of B molecules, r_B (nm)	2.5	See text
Radius of the cylindrical D sink, r_D (nm)	1	See text
Diffusion coefficient of A molecules in the bulk, D_A(m^2/s)	7.2×10^{-12}	See text
Diffusion coefficient of B molecules in the bulk, D_B(m^2/s)	8.6×10^{-12}	See text
Diffusion coefficient of A molecules along D sink, D_{AL}(m^2/s)	3×10^{-14}	[20,21]
Diffusion coefficient of B molecules along D sink, D_{BL}(m^2/s)	3×10^{-14}	[20,21]
Mean detrapping time of molecules from D sinks, $\tau_{A,B,C}$ (s)	0.3	[20,21]
Reaction factor for $A + B$ reaction in the bulk, γ_{AB}	2.8×10^{-4}	See text
Reaction factor for trapping of A and B on D sinks, γ_D	1.0	See text
Reaction factor for $A + B$ reaction on D sinks via 1D diffusion, γ_L	1.2×10^{-3}	See text
Reaction factor for $A + B$ reaction on D sinks via 3D diffusion, β	0.03	See text

complicated biomolecules such as proteins. Not all encounters of A and B result in formation of molecule C, therefore in Eq. (3) we introduced a factor $\eta_{AB} < 1$ that takes into account the following:

(i) The orientational constraints that two reactants must satisfy before forming the molecule C [34–42];

(ii) Influence of local rearrangements (surface diffusion, rotations, etc.) on reaction rate [35,36];

(iii) Intrinsic association rate due to free energy barrier separating final product C from the transient complex A-B formed by 3D diffusion [37–39].

In general the factor η_{AB} depends on temperature, molecule shapes, and location and size of specific reactive sites. A detailed discussion of the nature of η_{AB} is beyond the scope of this paper.

The electrostatic interaction energy between A and B molecules depends on the ionic strength of the buffer solution. Below we assume that the concentration of ions in electrolyte is much higher than the concentrations of A and B. For a monovalent electrolyte the Debye length is estimated as (see Table I)

$$l_D = \sqrt{\frac{\varepsilon_0 \varepsilon k_B T}{2 N_A e^2 C_{\rm buf}}} = 6 \text{ nm}, \tag{4}$$

where ε is the dielectric constant of the solution. The Debye length is comparable to the size of reactants; therefore the electrostatic interaction between A and B molecules is effectively screened and comes into play only at a short interparticle distances. Calculation of the electrostatic interaction in the buffer solution represents a separate task. Rather than going into such detail, we introduce a dimensionless electrostatic factor that accounts for the renormalization of the capture distance,

$$\lambda_{AB} = \left[r_0 \int_{r_0}^{\infty} \exp\left(\frac{U}{k_B T}\right) \frac{dr}{r^2} \right]^{-1}. \tag{5}$$

For ions A and B with the same charge $\lambda_{AB} < 1$. Finally, the reaction rate constant between A and B molecules is written in the form

$$\alpha_{AB} = 4\pi \gamma_{AB} (D_A + D_B)(r_A + r_B), \tag{6}$$

where we defined the total reaction factor $\gamma_{AB} = \eta_{AB} \lambda_{AB}$ that will be treated as an adjustable parameter in our model (see Table I). It should be noted that the reaction factor is a function of external parameters (temperature, ionic strength of the solution, dielectric constant of the solution, etc.) and local properties of reacting molecules (shape anisotropy, heterogeneous surface reactivity. etc.).

We are interested in the time dependence of the mean concentrations of A and B molecules. By integrating Eq. (1) over a volume containing a large number of D sinks, applying the divergence theorem, and dividing the result by this same volume we obtain

$$\frac{d\overline{C}_A}{dt} = -\alpha_{AB} \overline{C_A C_B} - \rho J_A, \tag{7}$$

where $\rho = C_D L_D$ is the total length of D sinks in a unit volume (an analog of the dislocation density in crystalline solids); C_D and L_D are the concentration and the length of D sinks, respectively. The overbar denotes the mean values. In the limit of low volume fraction occupied by reacting molecules and D sinks, $\overline{C_A C_B} \approx \overline{C}_A \overline{C}_B$. The net flux of A molecules J_A per unit length of D sinks can be represented in the form

$$J_A = J_A^+ - J_A^-, \tag{8}$$

where J_A^+ is the flux of molecules A which become trapped by D sinks and J_A^- is the flux of molecules A thermally released from D sinks, i.e., $J_A^- = n_A/\tau_A$, where n_A is the mean linear concentration of A molecules associated with D sinks and τ_A is the mean detrapping time (lifetime of a bound state of A molecule with D sink).

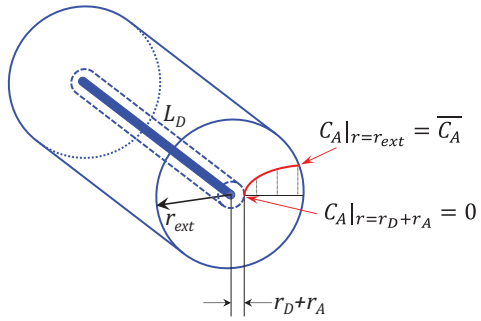

FIG. 2. (Color online) Capture volume around a D sink. A cylinder with radius r_{ext} is built around all D sinks such that the total volume of all cylinders equals the total solution volume. The concentrations of molecules A and B outside the cylinder are equal to their average values. These concentrations drop to zero at the D sink due to absorption on the sink.

A. Capture efficiency of D sinks

In this section we define the sink efficiency Z_A, the fundamental property of sink, and find the flux J_A^+,

$$Z_A = \frac{J_A^+}{D_A \overline{C}_A}. \tag{9}$$

First we assume that (i) linear concentrations of molecules trapped by D sinks are small; i.e., all sites at D sinks are available for incoming molecules A; and (ii) D sinks are sufficiently long, so that the influence of their edges on absorption of A and B molecules can be neglected. Consider a capture volume around a D sink (Fig. 2), defined by the cylinder of external radius r_{ext},

$$C_D L_D \pi r_{\text{ext}}^2 = \rho \pi r_{\text{ext}}^2 = 1. \tag{10}$$

Equation (10) states that all cylinders cover the entire volume under consideration. The radius of the cylindrical region r_{ext} has the meaning of a half distance between D sinks; i.e., at this distance the microscopic flux $\mathbf{j}_A \approx 0$.

After such a tessellation the flux J_A^+ can be found by solving the diffusion problem

$$div \mathbf{j}_A = 0, \tag{11}$$

$$\mathbf{j}_A = -D_A \nabla C_A - \frac{D_A C_A}{k_B T} \nabla E, \tag{12}$$

in the cylindrical region $r_A + r_D \leqslant r \leqslant r_{\text{ext}}$ (the capture volume). Here E is the electrostatic interaction energy of ions A with the D sink that in the case of DNA may have a charge distributed over the chain. The core of the sink is absorbing, resulting in the boundary condition

$$C_A|_{r=r_A+r_D} = 0. \tag{13}$$

At the outer boundary of the cylindrical region the concentration of molecules A equals the mean concentration (provided that the volume fraction occupied by reacting molecules and D sinks is low),

$$C_A|_{r=r_{\text{ext}}} = \overline{C}_A. \tag{14}$$

Assuming that the interaction energy E depends only on the cylindrical coordinate r we can find an analytic solution of Eqs. (11)–(14), from which we derive the flux

$$J_A^+ = 2\pi r D_A j_A|_{r=r_A+r_D} = Z_A D_A \overline{C}_A, \tag{15}$$

where Z_A is the capture efficiency of D sinks, according to the terminology adopted in materials science [30,31],

$$Z_A = 2\pi \left(\ln \frac{r_{\text{ext}}}{r_A + r_D} \right)^{-1} \lambda_D, \tag{16}$$

where the electrostatic reaction factor λ_D has the same meaning as the factor λ_{AB} in Eq. (5),

$$\lambda_D = \left[\int_{r_A+r_D}^{r_{\text{ext}}} \exp\left(\frac{E}{k_B T}\right) \frac{dr}{r} \right]^{-1} \ln \frac{r_{\text{ext}}}{r_A + r_D}. \tag{17}$$

Equation (11) is the quasisteady-state version of Eq. (1) in which we neglected the bimolecular reaction $A + B$ in the capture volume. This step implies two simplifying assumptions:

(i) Quasisteady-state approximation, which means that on the time scale of interest (decrease of mean concentrations $\overline{C}_{A,B}$) the instantaneous rates of change of local concentrations in the vicinity of the D sink are approximately equal to zero;

(ii) Trapping of molecules by D sinks and bimolecular reaction contribute additively to the rate of change of mean concentrations.

It should be noted that Eq. (16) is valid in the case of long D sinks $L_D \gg r_{\text{ext}}$. If the length of D sinks is small compared to the average spacing between D sinks $L_D \ll 1/\sqrt[3]{C_D}$, then the D sink can be represented by a prolate spheroid. Without the interaction of A ions with the D sink the capture efficiency of the prolate spheroid is given by [43,44]

$$\begin{aligned} Z_A &= 2\pi \frac{2\sqrt{1-u^2}}{\ln[(1+\sqrt{1-u^2})/(1-\sqrt{1-u^2})]} \\ &\approx 2\pi \left(\ln \frac{L_D}{r_A + r_D} \right)^{-1}, \\ u &= \frac{2(r_A + r_D)}{L_D}. \end{aligned} \tag{18}$$

Combining the results of this section we will use the following interpolation formula:

$$Z_A(L_D) = \eta_D \lambda_D \begin{cases} \frac{4\pi\sqrt{1-u^2}}{\ln[(1+\sqrt{1-u^2})/(1-\sqrt{1-u^2})]}, & L_D \leqslant 1/\sqrt[3]{\pi C_D} \\ 2\pi \left(\ln \frac{r_{\text{ext}}}{r_A + r_D} \right)^{-1}, & L_D > 1/\sqrt[3]{\pi C_D} \end{cases}. \tag{19}$$

The trapping of a molecule A occurs upon its diffusive encounter with the D sink provided both of them have favorable orientations; therefore in Eq. (19) we introduced the factor η_D, similar to the bimolecular reaction in the bulk [see Eq. (3)]. Again the factor $\gamma_D = \eta_D \lambda_D$ is considered to be the fitting parameter. Figure 3 shows the dependence of the "geometrical" capture efficiency on D sink length.

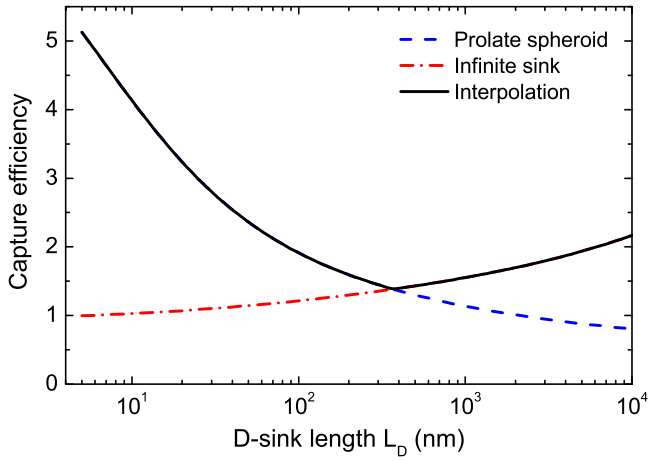

FIG. 3. (Color online) The geometrical capture efficiency $z_A = Z_A/\eta_D\lambda_D$ as a function of D-sink length L_D [Eq. (19), solid line]. Concentration of D sinks $C_D = 10\,\mathrm{n}M$; other parameters are listed in Table I. Dash-dotted and dashed lines correspond to Eqs. (16) and (18), respectively.

Now we can write the rate of A molecule loss per unit length of D sinks,

$$J_A^+ = Z_A(D_A + D_D)\overline{C}_A\left(1 - \sum_{i=A,B,C} 2r_i n_i\right) + \beta_A Z_A(D_A + D_D)\overline{C}_A 2r_B n_B, \quad (20)$$

where the diffusion coefficient D_D is introduced to account for the mobility of short D sinks (see Sec. III). In Eq. (20) we distinguish two mechanisms of molecule trapping by D sinks. The first term on the right-hand side is the diffusion flux of A molecules to the unit length of D sinks; the multiple $(1 - \sum_{i=A,B,C} 2r_i n_i)$ accounts for a fraction of D sinks occupied by A, B, and C molecules (crowding effect). The second term is the diffusion flux of A molecules landing directly to B molecules which occupy the fraction of D sink $2r_B n_B$; β_A is the reaction factor for the in-place association of neighboring A and B molecules (it can be viewed as a probability of collisions with the suitable orientations for C molecule formation). In the following it is assumed that $\beta_A = \beta_B = \beta$. The reaction of $A(B)$ molecules diffusing from the solution to $B(A)$ molecules trapped on D sinks is similar to 3D bimolecular reaction (6) in solution. This reaction pathway can be efficient if the linear charge of D sink neutralizes the electrostatic repulsion between free $A(B)$ molecules and trapped $B(A)$ molecules.

B. Bimolecular reaction on one-dimensional sink

The objective of this section is to find the reaction rate of A and B molecules on a D sink during one-dimensional diffusion and to construct the rate equations for the mean linear concentrations,

$$n_{A,B}(t) = \frac{1}{L_D}\int_{L_D} s_{A,B}(x,t)dx, \quad (21)$$

where $s_{A,B}(x,t)$ are concentrations of A and B molecules on a D sink at position x. To this end we use the mean-field approach as well. Molecules A arriving to D sinks undergo a 1D random walk until they escape thermally from D sinks or locate reaction partners. At the same time molecules B can land directly to trapped A molecules [compare with Eq. (20)]. The rate equation for the mean linear concentration of molecules A reads

$$\frac{dn_A}{dt} = Z_A(D_A + D_D)\overline{C}_A\left(1 - \sum_{i=A,B,C} 2r_i n_i\right) - \beta Z_B(D_B + D_D)\overline{C}_B 2r_A n_A - R_{AB} - \frac{n_A}{\tau_A}, \quad (22)$$

where R_{AB} is the reaction rate between A and B molecules as a result of their encounters during 1D diffusion along the D sink.

To find R_{AB} we will use the approach of Hardt [23], based on the conjecture that at a steady state the rate of diffusional encounters between the two reacting partners equals the sum of the encounter rates of two independent processes. These independent rates are obtained by alternately immobilizing one of the reaction partners while the other partner diffuses freely. Hardt [23] showed that unlike the Smoluchowski classical approach [33], this principle allowed one to obtain the steady-state reaction rates for all dimensionalities in a unified fashion. Also, convincing arguments are presented as to why the Smoluchowski method [33] of evaluating the rate of bimolecular reaction in 3D space is not suitable for the 1D case. Smoluchowski replaced the real system with two migrating species of molecules by an imaginary system in which one of the species is immobile and the other is diffusing freely with an increased diffusion coefficient $D_A + D_B$. In the Smoluchowski model the immobile molecules are acting as sinks for the diffusing molecules. Hence the reaction rate is defined as the flux of diffusing molecules to sinks. In 3D space the reaction rate is independent of the choice of immobile particles in the imaginary system. The justification of the Smoluchowski method for using the sum of the diffusion coefficients as the diffusion coefficient for the diffusing reactant can be found in [45], where the kinetics of the diffusion limited reaction $A + B$ was considered in terms of the pair probability densities of the reacting particles. The application of the Smoluchowski method in one or in two dimensions leads to conceptual difficulties [23]. For example, it turns out that the reaction rate is crucially dependent on which reaction species is to be immobilized in the imaginary system [23].

Since the movements of individual molecules are mutually independent, it is reasonable to expect that the process in which two particles accidentally meet can be expressed as the sum of two independent processes—the diffusion of A molecules while B molecules are immobilized, and the diffusion of B molecules while A molecules are immobilized. Therefore, following [23] the reaction rate is written as

$$R_{AB} = \gamma_L(n_A I_B + n_B I_A), \quad (23)$$

where I_A is the flux of diffusing molecules A into one immobilized molecule B and I_B is the flux of diffusing molecules B into one immobilized molecule A. Similar to the 3D case, in Eq. (23) we introduced the reaction factor γ_L for the reaction $A + B$ on a D sink.

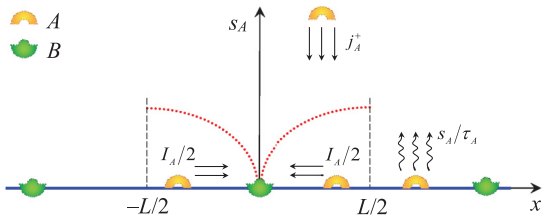

FIG. 4. (Color online) Bimolecular reaction on an infinitely long D sink. Due to symmetry considerations we consider only a region between $-L/2$ and $L/2$. Molecules B are assumed to be immobile. Molecules A are trapped from the solution (j_A^+) and evaporate back to the solution (s_A/τ_A). While on the sink, a molecule A can encounter a molecule B due to 1D diffusion from both sides ($I_A/2$). The dotted red line shows the concentration profile $s_A(x,t)$ of molecules A on the sink.

To find the flux I_A consider a D sink containing trapped B molecules, which are distributed uniformly with the spacing $L = 1/n_B$ (Fig. 4). Let us assume for now that B molecules trapped at D sink are immobile. The microscopic linear concentration of A molecules $s_A(x,t)$ in the region $0 \leqslant x \leqslant L/2$ obeys the diffusion equation

$$\frac{\partial s_A}{\partial t} = j_A^+ - \frac{s_A}{\tau_A} + D_{AL}\frac{\partial^2 s_A}{\partial x^2}, \tag{24}$$

with the absorbing boundary condition at $x = 0$ that corresponds to reaction between A and B molecules,

$$s_A(0,t) = 0, \tag{25}$$

and reflecting boundary condition at the symmetry point $x = L/2$,

$$\left.\frac{\partial s_A(x,t)}{\partial x}\right|_{x=L/2} = 0. \tag{26}$$

In Eq. (24) D_{AL} represents the 1D diffusion coefficient of molecules A along D sinks; j_A^+ is the flux of A molecules to the unoccupied piece of D sink.

To find the dependence of $s_A(x,t)$ on x we assume that after a short initial transient period a quasisteady state establishes. This means that $s_A(x,t)$ adiabatically adjusts to $\overline{C}_{A,B}$, the slowly varying mean concentrations of molecules in the solution,

$$j_A^+ - \frac{s_A}{\tau_A} + D_{AL}\frac{\partial^2 s_A}{\partial x^2} = 0. \tag{27}$$

The solution of Eq. (27) in the region $0 \leqslant x \leqslant L/2$ is [46,47]

$$s_A(x) = j_A^+\tau_A\left\{1 - \frac{\cosh[(x - L/2)(\sqrt{D_{AL}\tau_A})^{-1}]}{\cosh[L(2\sqrt{D_{AL}\tau_A})^{-1}]}\right\}. \tag{28}$$

The mean concentration on the linear sink [see Eq. (21)] is given by

$$n_A = j_A^+\tau_A\left\{1 - 2\frac{\sqrt{D_{AL}\tau_A}}{L}\tanh\left(\frac{L}{2\sqrt{D_{AL}\tau_A}}\right)\right\}. \tag{29}$$

The total flux of molecules A to the molecule B from both sides (Fig. 4) is written as

$$I_A = -2D_{AL}\left.\frac{ds_A(x)}{dx}\right|_{x=0} = 2j_A^+\tau_A\sqrt{\frac{D_{AL}}{\tau_A}}\tanh\left(\frac{L}{2\sqrt{D_{AL}\tau_A}}\right). \tag{30}$$

To obtain a self-consistent expression for R_{AB} in terms of the D sink parameters and the mean linear concentrations, L is replaced with $1/n_B$ and $j_A^+\tau_A$ is eliminated from Eq. (30) using Eq. (29),

$$I_A = 2n_A\sqrt{\frac{D_{AL}}{\tau_A}}\frac{\tanh[(2n_B\sqrt{D_{AL}\tau_A})^{-1}]}{1 - 2n_B\sqrt{D_{AL}\tau_A}\tanh[(2n_B\sqrt{D_{AL}\tau_A})^{-1}]}. \tag{31}$$

The expression for I_B can be obtained by interchanging the labels A and B in Eq. (31).

It is instructive to analyze the reaction rate R_{AB} in simple limiting cases.

(I) In the limiting case $n_B\sqrt{D_{AL}\tau_A} \ll 1$ and $n_A\sqrt{D_{BL}\tau_B} \ll 1$ we obtain

$$R_{AB} = 2\left(\sqrt{\frac{D_{AL}}{\tau_A}} + \sqrt{\frac{D_{BL}}{\tau_B}}\right)n_A n_B\gamma_L; \tag{32}$$

i.e., the reaction obeys classical second-order kinetics $n_A n_B$. In this limiting case the particle detrapping is much faster than the bimolecular reaction. Reaction rate (32) is equivalent to the corresponding result of Suna [48], where the kinetics of exciton-exciton annihilation was considered using the formalism of two-particle distribution function. A similar result was derived by Molski [26] in the framework of the fluctuation dissipation theory for the steady-state 1D bimolecular annihilation $A + A \to 0$ accompanied by unimolecular decay $A \to 0$ (in our system unimolecular decay is equivalent to particle detrapping from D sinks).

(II) In the limiting case $n_B\sqrt{D_{AL}\tau_A} \gg 1$ and $n_A\sqrt{D_{BL}\tau_B} \gg 1$ the bimolecular process dominates detrapping of molecules:

$$R_{AB} = 12(D_{AL}n_B + D_{BL}n_A)n_A n_B\gamma_L. \tag{33}$$

Exactly the same reaction rate (without the parameter γ_L) was derived in [23] using rather simple arguments. Moreover, the similar result was found using the fluctuation dissipation theory [26]. Note in Eq. (33) the terms proportional to $n_A n_B^2$ and $n_A^2 n_B$ indicating that the reaction kinetics is of nonclassical third order. The Monte Carlo simulation of an elementary reaction $A + A$ in a linear lattice without detrapping also revealed the third-order reaction kinetics [24,29]. In this limiting case trapped molecules have a potential to migrate to distances larger than the average distance between trapped molecules. During an encounter of a reactant with its reaction partner molecule C may form with a certain probability lower than unity. This implies that the reactant may reflect from or migrate further through its partner (so to speak, along the other side of DNA, if we take into account the spatial structure of DNA). The probability to form molecule C is controlled by the reaction factor γ_L.

Both limiting cases, Eqs. (32) and (33), can be checked using rather simple physical reasoning. The diffusion length, i.e., the average distance a trapped molecule can cover before detrapping, is about $x_i \sim \sqrt{D_i \tau_i}, i = A,B$. In the first limiting case the diffusion length of molecules is smaller than the mean distance between the reaction partners $x_A n_B = x_A/L_B \ll 1$ and $x_B n_A = x_B/L_A \ll 1$. In this case only molecules situated within the diffusion length near their reaction partners can reach each other. Hence, the fluxes $I_{A,B}$ and the reaction rate R_{AB} are estimated as

$$I_A \sim D_{AL}\frac{n_A}{x_A} = \sqrt{\frac{D_{AL}}{\tau_A}}n_A \quad \text{and} \quad I_B \sim D_{BL}\frac{n_B}{x_B} = \sqrt{\frac{D_{BL}}{\tau_B}}n_B, \tag{34}$$

$$R_{AB} \sim \left(\sqrt{\frac{D_{AL}}{\tau_A}} + \sqrt{\frac{D_{BL}}{\tau_B}}\right) n_A n_B. \tag{35}$$

In the second limiting case, formally, the diffusion lengths are larger than the mean distances between trapped molecules $\sqrt{D_{AL}\tau_A} \gg 1/n_B$ and $\sqrt{D_{BL}\tau_B} \gg 1/n_A$. One cannot use the diffusion lengths in estimation of concentration gradients. Instead, the mean distance $L_i = n_i^{-1}$ between trapped molecules should be used,

$$I_A \sim D_{AL}\frac{n_A}{n_B^{-1}} = D_{AL} n_A n_B \quad \text{and} \quad I_B \sim D_{BL}\frac{n_B}{n_A^{-1}} = D_{BL} n_A n_B. \tag{36}$$

In this case the reaction rate R_{AB} is proportional to

$$R_{AB} \sim (D_{AL} n_B + D_{BL} n_A) n_A n_B. \tag{37}$$

Equations (35) and (37) demonstrate the same concentration dependence as 1D reaction rates (32) and (33), respectively.

C. Rate equations

To summarize the discussions of the previous sections we write the set of ordinary differential equations (ODEs) for reactant concentrations and the reaction product concentration,

$$\frac{d\overline{C}_A}{dt} = -\alpha_{AB}\overline{C}_A\overline{C}_B - Z_A\rho(D_A + D_D)\overline{C}_A\left(1 - \sum_{i=A,B,C} 2r_i n_i\right) - \beta Z_A \rho (D_A + D_D)\overline{C}_A 2r_B n_B + \rho\frac{n_A}{\tau_A}, \tag{38}$$

$$\frac{d\overline{C}_B}{dt} = -\alpha_{AB}\overline{C}_A\overline{C}_B - Z_B\rho(D_B + D_D)\overline{C}_B\left(1 - \sum_{i=A,B,C} 2r_i n_i\right) - \beta Z_B \rho (D_B + D_D)\overline{C}_B 2r_A n_A + \rho\frac{n_B}{\tau_B}, \tag{39}$$

$$\frac{d\overline{C}_C}{dt} = \alpha_{AB}\overline{C}_A\overline{C}_B - Z_C\rho(D_C + D_D)\overline{C}_C\left(1 - \sum_{i=A,B,C} 2r_i n_i\right) + \rho\frac{n_C}{\tau_C}, \tag{40}$$

$$\frac{dn_A}{dt} = Z_A(D_A + D_D)\overline{C}_A\left(1 - \sum_{i=A,B,C} 2r_i n_i\right) - \beta Z_B (D_B + D_D)\overline{C}_B 2r_A n_A - \gamma_L(n_A I_B + n_B I_A) - \frac{n_A}{\tau_A}, \tag{41}$$

$$\frac{dn_B}{dt} = Z_B(D_B + D_D)\overline{C}_B\left(1 - \sum_{i=A,B,C} 2r_i n_i\right) - \beta Z_A (D_A + D_D)\overline{C}_A 2r_B n_B - \gamma_L(n_A I_B + n_B I_A) - \frac{n_B}{\tau_B}, \tag{42}$$

$$\frac{dn_C}{dt} = Z_C(D_C + D_D)\overline{C}_C\left(1 - \sum_{i=A,B,C} 2r_i n_i\right) - \frac{n_C}{\tau_C} + \gamma_L(n_A I_B + n_B I_A) + \beta Z_A (D_A + D_D)\overline{C}_A 2r_B n_B + \beta Z_B (D_B + D_D)\overline{C}_B 2r_A n_A, \tag{43}$$

Initial conditions for the set of ODEs (38)–(43) are

$$\overline{C}_A\big|_{t=0} = C_{A0}, \quad \overline{C}_B\big|_{t=0} = C_{B0}, \tag{44}$$

$$\overline{C}_C\big|_{t=0} = 0, \tag{45}$$

$$n_i|_{t=0} = 0, \quad i = A,B,C. \tag{46}$$

The time dependence of the total concentration of molecules C, the reaction product, is given by

$$C_C^{\text{total}}(t) = \overline{C}_C(t) + \rho n_C(t). \tag{47}$$

For the purpose of this paper it is instructive to distinguish three reaction pathways. The direct summation of Eqs. (40) and (43) yields

$$\begin{aligned}\frac{dC_C^{\text{total}}}{dt} &= \frac{d\overline{C}_C}{dt} + \rho\frac{dn_C}{dt} \\ &= \alpha_{AB}\overline{C}_A\overline{C}_B + \rho\gamma_L(n_A I_B + n_B I_A) \\ &\quad + 2\beta\rho[Z_A(D_A + D_D)\overline{C}_A r_B n_B \\ &\quad + Z_B(D_B + D_D)\overline{C}_B r_A n_A].\end{aligned} \tag{48}$$

The right-hand side of Eq. (48) contains three contributions to the reaction rate:

(i) Reaction in the solution,

$$\left(\frac{dC_C^{\text{total}}}{dt}\right)_{3D-\text{bulk}} = \alpha_{AB}\overline{C}_A\overline{C}_B; \tag{49}$$

(ii) formation of C molecules due to 3D diffusion of A and B molecules from the solution to their partners trapped by D sinks,

$$\left(\frac{dC_C^{\text{total}}}{dt}\right)_{3D-\text{sink}} = 2\beta\rho[Z_A(D_A+D_D)\overline{C}_A r_B n_B + Z_B(D_B+D_D)\overline{C}_B r_A n_A]; \tag{50}$$

(iii) formation of C molecules on D sinks via 1D diffusion and association of A and B molecules trapped by D sinks,

$$\left(\frac{dC_C^{\text{total}}}{dt}\right)_{1D} = \rho\gamma_L(n_A I_B + n_B I_A). \tag{51}$$

Correspondingly, the total concentration of C molecules consists of three contributions,

$$C_C^{\text{total}} = C_{3D-\text{bulk}} + C_{3D-\text{sink}} + C_{1D}, \tag{52}$$

which are found by integration when the solution of Eqs. (38)–(46) is obtained,

$$C_{3D-\text{bulk}}(t) = \alpha_{AB}\int_0^t \overline{C}_A(t')\overline{C}_B(t')dt', \tag{53}$$

$$C_{3D-\text{sink}}(t) = 2\beta\rho\int_0^t [Z_A(D_A+D_D)\overline{C}_A r_B n_B + Z_B(D_B+D_D)\overline{C}_B r_A n_A]dt', \tag{54}$$

$$C_{1D}(t) = \rho\gamma_L\int_0^t (n_A I_B + n_B I_A)dt'. \tag{55}$$

The contribution of each reaction mechanism depends on kinetic parameters and, in particular, on interplay between reaction factors γ_{AB}, γ_D, γ_L, and β.

III. NUMERICAL SIMULATION AND DISCUSSION

The ODE set, Eqs. (38)–(46), can be solved numerically with a standard code for stiff systems. We used the RADAU code based on the implicit Runge-Kutta method of variable order with an adaptive time-step control [49].

As mentioned above, we applied our model to describe the experimental system consisting of reacting streptavidin (A) and biotin (B) in buffer solution with addition of DNA segments of various concentrations (Fig. 5). All species present in the solution are charged: A and B molecules have positive charges $8e$ and $4e$, respectively; DNA segments have negative charge, $-2e$ per base pair (bp).

Molecular radii of A and B were estimated as hydrodynamic radii corresponding to a protein of 60 kDa (modified streptavidin) and PEG5000 [biotin, functionalized with 100-unit polyethylene glycol (PEG)], respectively. Three-dimensional diffusion coefficients of these reactants were calculated using

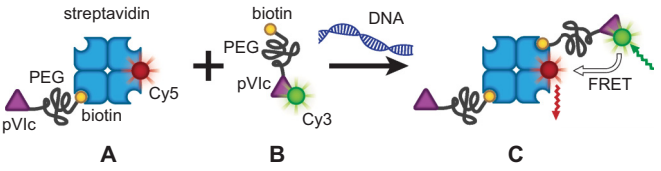

FIG. 5. (Color online) Schematic of the experimental system. Streptavidin (A) and biotin (B) are rendered able to slide along DNA by functionalizing them with a peptide sled pVIc via a 100-unit PEG linker. DNA of different lengths and concentrations is used in solution as a catalyst for the reaction, whose progress is monitored in time by detecting the FRET signal arising from the reaction product C.

the Stokes-Einstein equation,

$$D_{A,B} = \frac{k_B T}{6\pi\mu r_{A,B}}, \tag{56}$$

where μ is the dynamic viscosity of the solution.

One-dimensional diffusion coefficients of bare pVIc and pVIc with various cargoes were measured using direct single-molecule observations of fluorescently labeled peptides and proteins [20,21]. For our simulations, the 1D diffusion coefficients were adjusted for the dynamic viscosity of the high-glycerol buffer solution that was used in our experiments [22]. The detrapping times were estimated in the same study [20,21]; we assumed them to be the same for all molecular species. The parameters that were used in the simulation are listed in Table I.

The experimental reaction time is defined as a constant τ, obtained from fitting the FRET trace with the exponential function $C(t) = C_{\max}[1-\exp(-t/\tau)]$ [22]. In our theoretical modeling this time τ corresponds to the time when the product concentration reaches ~63% of its maximum value.

The fitting parameters of our model are the reaction factors. As a first step in the numerical simulation, the "bulk" reaction factor γ_{AB} was adjusted to yield the experimentally observed average reaction time in solution without DNA (see Fig. 6). Regarding the seemingly low bulk reaction factor $\gamma_{AB} = 2.8\times 10^{-4}$, the electrostatic repulsion at short distances, despite the

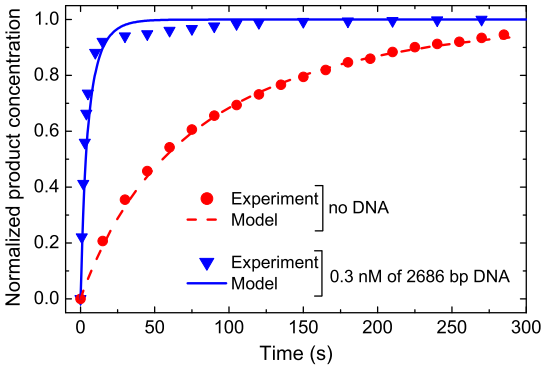

FIG. 6. (Color online) Time dependence of the reaction product concentration $C_C(t)$ in the system with and without D sinks as obtained from the experiments and theoretical modeling. Time interval between data points was 1 s; here only a selection of experimental data is shown.

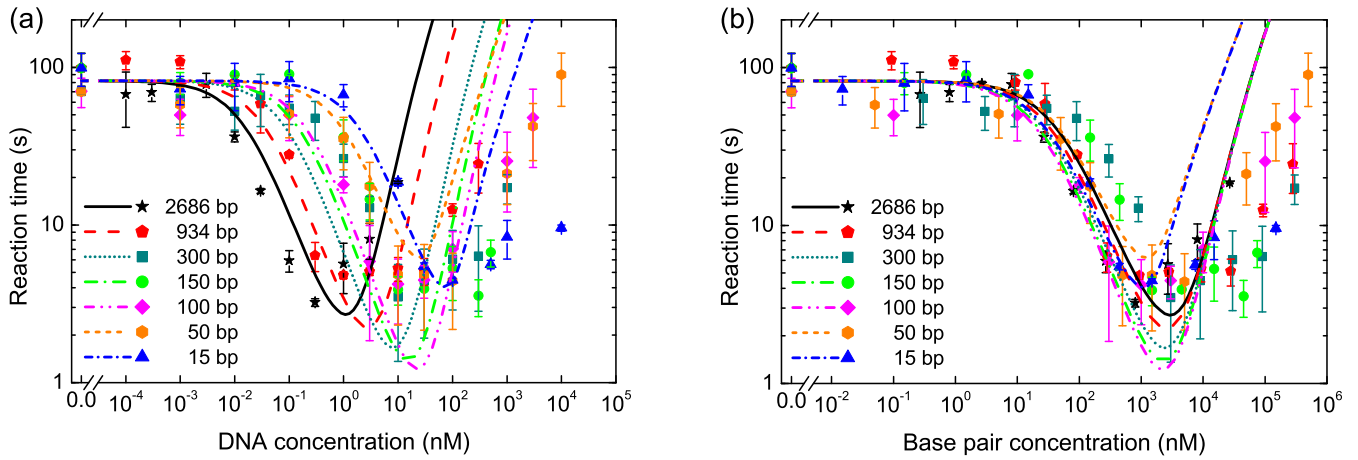

FIG. 7. (Color online) Biotin-streptavidin reaction speedup in the presence of DNA. The fitting parameters γ_i and β were the same for all the curves. The diffusion coefficient $D_D = 0$ for DNA segments longer than 50 bp. In the case of short DNA segments, 15 and 50 bp, calculations were performed with 1D diffusion coefficients $D_{AL} = D_{BL}$ and $D_D \neq 0$ [see Eq. (57)]. A separate model for short DNA fragments is discussed in the Appendix. (a) The experimental data describing the dependence of the reaction time on DNA concentration for different DNA lengths are compared to the model. (b) Both experimental and model data on the reaction time are replotted as a function of DNA base pair concentration.

screening by electrolyte ions, is responsible for such a low value.

The next step is to adjust the reaction factors γ_D, γ_L, and β in case DNA is present in the solution. Their choice is not unique, though there are certain physical constraints related to electrostatic interactions. DNA attracts A and B molecules, but only at short distances of ~6 nm [see Eq. (4)]. Therefore it is reasonable to assume that the reaction factor for trapping by D sinks is about unity. DNA neutralizes charges of trapped A and B molecules; however, at small distances one can expect a repulsive interaction between them; in addition, A and B molecules must have specific spatial orientations for the association reaction. For these reasons the reaction factor for association on D sink γ_L should be smaller than unity. The same conclusion is valid for the reaction factor β. The molecule landing from the solution to the reaction partner has more freedom to adjust itself for the association as compared to reaction between A and B both trapped to D sink; therefore one can expect that $\beta > \gamma_L$. The final set of parameters γ_D, γ_L, and β (Table I) used for comparison of model predictions with experimental data satisfies the requirements discussed above. Note also that $\beta\gamma_D/\gamma_{AB} \sim 100 \gg 1$, which is in agreement with electrostatic arguments.

Figure 7 shows that a good correspondence between experimental data and model predictions can be reached as a result of fitting. Experimentally we observed that the reaction acceleration is controlled largely by the absolute concentration of DNA base pairs, rather than by DNA fragment length and concentration separately. Figure 7(b) demonstrates clustering of the experimental data points plotted against the DNA base pair concentration that is proportional to ρ. Similar to the experimental data points, the clustering of model curves is observed [Fig. 7(b)], confirming our experimental observations. It should be stressed that we obtained a unified description of the experimental system using the same set of fitting parameters for all lengths of DNA fragments. What is remarkable is that the minimum reaction time is achieved in the same base pair concentration range 10^{-3}–10^{-4} nM for all DNA lengths.

In our previous study we also observed reaction acceleration in the solution with DNA fragments as short as 5 nm (15 bp) and 16.7 nm (50 bp). In these cases one can hardly speak of 1D diffusion along DNA fragments whose length is comparable to the sizes of A and B molecules. This case is considered separately in the Appendix taking into account the diffusion mobility of short DNA fragments. However, the model of this section works well even for short DNA fragments (see Fig. 7) if we set 1D diffusion coefficients to zero and take the mobility of short DNA fragments into account, estimating their diffusion coefficient by approximating a cylindrical segment loaded with an $A(B)$ molecule by a sphere of the same volume

$$D_D = \frac{k_B T}{6\pi\mu}\left(\frac{3}{4}r_D^2 L_D + r_A^3\right)^{-1/3} \approx D_{A,B}, \quad L_D < 16.7\,\text{nm}. \tag{57}$$

Note that for D sink lengths in the range of 100–2686 bp the minimum of the curve $\tau(\rho)$ in Fig. 7(b) becomes deeper with decreasing D sink length. In the model equations the dependence on D sink length appears in Eq. (19) for the D sink efficiency. If one neglects this dependence then curves $\tau(\rho)$ [Fig. 7(b)] for all D sink lengths would collapse into a single curve.

It is of great interest to quantitatively evaluate the contributions of reaction mechanisms (53)–(55) to the reaction kinetics. The ODE set, Eqs. (38)–(46), was solved numerically until the end of the reaction. Then integrals in Eqs. (53)–(55) were evaluated. Figure 8 shows the contribution of each reaction mechanism normalized to the final concentration of the reaction product $C_C^{\text{total}}(t \gg \tau) = \min(C_{A0}, C_{B0})$ when the reaction is completed. It is seen that at DNA concentrations in the vicinity of the minimum reaction time the contribution of the 1D reaction mechanism is the highest; it reaches the value of about 90% [Figs. 8(b) and 8(d)]. According to Fig. 8(d), in the whole range of DNA concentration the 1D mechanism

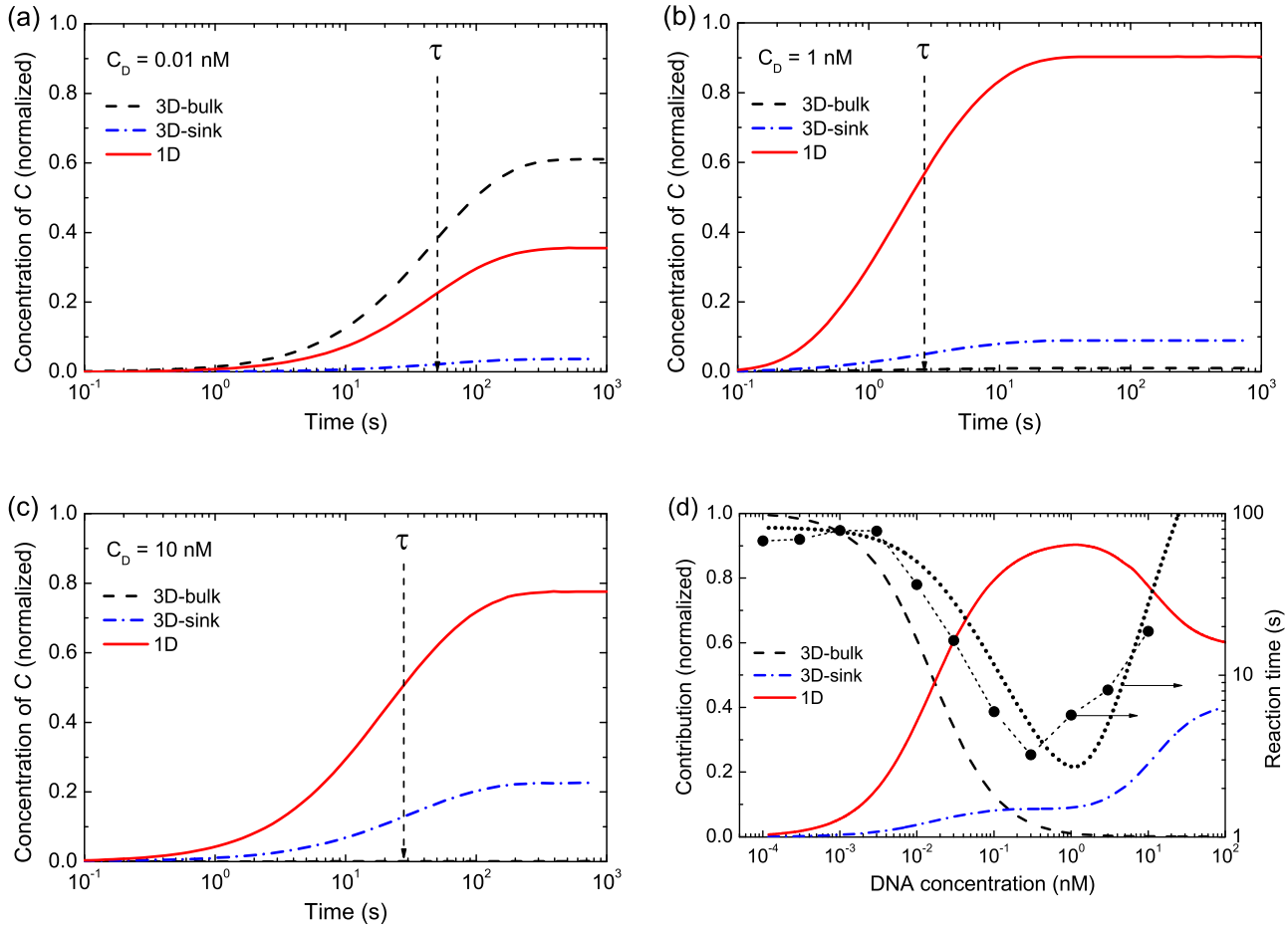

FIG. 8. (Color online) Reaction mechanism contributions normalized to the final concentration of the reaction product. The length of D-sink segments is 2686 bp; $D_D = 0$. (a–c) The time dependence of the contributions given by Eqs. (53)–(55) for D-sink concentrations 0.01, 1, and 10 nM, respectively; τ is the reaction time defined in the text. (d) DNA concentration dependence of reaction mechanism contributions $C_\alpha/C_C^{\text{total}}$ ($\alpha = 3D - \text{bulk}$, $3D - \text{sink}$, $1D$) when the reaction is completed ($t \gg \tau$). The model dependence of the reaction time on DNA segment concentration (dotted black line) is shown in the logarithmic scale (right y axis). Symbols refer to experimental data.

dominates over the 3D-sink mechanism. Thus, our model supports the hypothesis that 1D diffusion *per se* can indeed provide a kinetic advantage for bimolecular associations.

To investigate the reaction acceleration that can be achieved and its sensitivity to the parameters, we studied the dependence of the reaction time on DNA concentration for different values of 1D diffusion coefficients (D_{AL}, D_{BL}) and detrapping times ($\tau_A = \tau_B = \tau_C$). Figure 9 shows the effect of changing the parameters over several orders of magnitude.

Recent single-molecule experiments revealed that the diffusion coefficients for 1D sliding along DNA are two or more orders of magnitude lower than the 3D diffusion coefficients [20,21,51–53]. Previously it was often assumed that for reaction acceleration by reduction of dimensionality to occur, the 1D diffusion coefficients have to be higher or of the same order of magnitude as the related 3D diffusion coefficients [54]. However, in our model the speeding-up effect is significant even in case D_{AL} and D_{BL} are a factor of 10^3 less than the corresponding 3D diffusion coefficients [Figs. 9(a) and 9(b)]. Inspecting our simulation results we found that in the range of DNA concentrations where the reaction acceleration is observed, the 1D reaction mechanism is of the third order; i.e., it is described well by Eq. (33). We believe that the third order of the 1D reaction kinetics is the reason why at optimum DNA concentrations the system prefers the 1D reaction pathway notwithstanding relatively low 1D diffusivity. Figure 9(b) shows the reaction mechanism contributions to the reaction kinetics as a function of relative "strength" of 1D diffusion $x = D_{AL}/D_A = D_{BL}/D_B$. Here we scaled both 1D diffusion coefficients in the same manner. When we set D_{BL} to zero and varied only D_{AL}, we obtained a figure very similar to Fig 9(b).

Decreasing the detrapping time of the reactants results in a decrease of the acceleration effect [Fig. 9(c)]. This is caused by the fact that chances of reactants to find each other on DNA decrease due to small detrapping (residence) times ($\tau_A \ll 1$ s). It is important to note that varying the detrapping time of the reactants influences not only the acceleration effect itself, but also the position of the reaction time minimum as a function of DNA concentration. At high detrapping times reaction acceleration is observed at lower DNA concentrations as compared to the cases with low detrapping times. The reason behind it is that increasing the detrapping times increases the probability of reactants to meet each other on the DNA

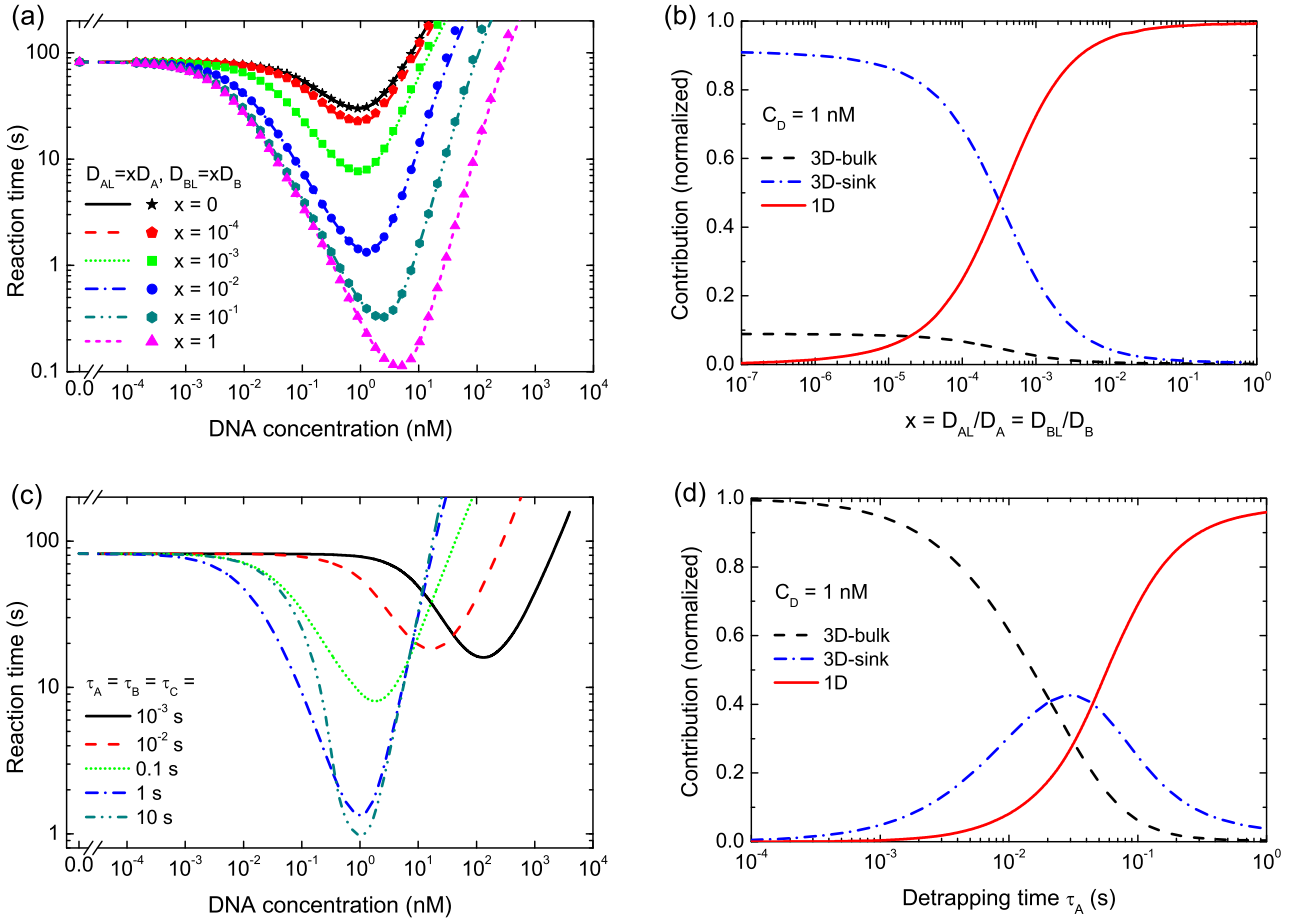

FIG. 9. (Color online) Influence of 1D diffusion coefficients and detrapping times on reaction kinetics. The length of D-sink segments is 2686 bp; $D_D = 0$. (a) Dependence of the reaction time on 1D diffusion coefficients. Curves correspond to the solution of Eqs. (38)–(43) with the 1D reaction rate given by Eqs. (23) and (31); symbols correspond to calculations with the third-order reaction rate (33). (b) Reaction mechanism contributions normalized to the final concentration of the reaction product $C_\alpha/C_C^{\text{total}}$ ($\alpha = 3D - \text{bulk}, 3D - \text{sink}, 1D$) when the reaction is completed ($t \gg \tau$) as a function of relative strength of 1D diffusion $x = D_{AL}/D_A = D_{BL}/D_B$. The D-sink concentration is selected in the vicinity of the reaction time minimum for D-sink segments of 2686 bp [Fig. 7(a), solid black line]. (c) Dependence of the reaction time on DNA concentration at several values of the detrapping time. (d) Reaction mechanism contributions normalized to the total concentration of the reaction product $C_\alpha/C_C^{\text{total}}$ ($\alpha = 3D - \text{bulk}, 3D - \text{sink}, 1D$) when the reaction is completed ($t \gg \tau$) as a function of detrapping time at $C_D = 1\,\text{n}M$. The parameters that were varied are indicated in the figures; other input parameters are kept the same as in previous calculations.

molecule they both are bound to. However, increasing the DNA concentration in this case only decelerates the reaction because the reactants become effectively separated from each other due to increased chances for them to be attached to different DNA molecules with low probability of escaping to the solution (high detrapping times). Figure 9(d) shows the dependence of reaction mechanism contributions on the detrapping time. It is seen that at sufficiently high detrapping times $\tau_A > 0.1$ s the 1D reaction mechanism dominates all other reaction pathways.

IV. SUMMARY

In this study we developed a phenomenological model that describes the kinetics of a bimolecular reaction in solution that utilizes both 3D and 1D reaction pathways. We used the mean-field approach to construct the chemical rate equations for mean concentrations of reacting species both in the solution and on extended 1D traps. The main features of the model are as follows:

(1) Reaction rate constants were derived in a quasisteady-state approximation assuming that mean concentrations change on a time scale larger than that of local concentrations in the vicinity of D sinks;

(2) Trapping and association of reactants at D sinks and reaction in the bulk were assumed to contribute additively to the rate of change of mean concentrations;

(3) Electrostatic interaction, orientational, and intrinsic constraints for reaction were taken into account by introduction of the reaction factors that are adjusted to fit model calculations to our experimental results;

(4) The bimolecular reaction between trapped reactants exhibits the nonclassical third-order behavior when trapping by 1D sinks is essential (i.e., in the optimal acceleration regime);

(5) Third-order kinetics renders the 1D reaction efficient even at small 1D diffusion coefficients of the reactants (compared to the corresponding 3D diffusion coefficients).

The dependence of the reaction kinetics on the main reaction parameters was investigated. The model distinguishes three reaction mechanisms: (i) homogeneous reaction in the solution via 3D diffusion; (ii) 3D mechanism of bimolecular reaction enhanced by electrostatic interaction with sinks; and (iii) combination of 3D search of a linear sink, electrostatic interaction with it, and 1D search of a reaction partner trapped on the same linear sink. The contributions of these mechanisms to the formation of the reaction product were evaluated. As a limiting case of the model we also considered the bimolecular reaction in solution with mobile molecular traps of similar size as reactants. In this case the mobility of molecular traps and electrostatic interaction with reacting molecules are essential. The criteria were found when molecular traps catalyze the reaction between reactants.

We applied our model to the experimental data from our studies of the association kinetics between biotin and streptavidin molecules, which were functionalized by DNA-sliding peptides, in a solution with DNA. The behavior of such a complex multicomponent biochemical system was described in a semiquantitative manner. The model reproduces all our experimental observations well. According to our simulations the contribution of 1D diffusion to the reaction kinetics is substantial. At DNA concentrations in the vicinity of the minimum reaction time the relative contribution of 1D reaction mechanism reaches the value of about 90%.

Our model can be adapted to provide insights into the systems with coupled 3D and 1D diffusion that are frequently observed in biology. The most studied examples of these systems are search processes on DNA, such as repressor-operator interactions, endonuclease-restriction site search, DNA-repair proteins searching for damage, and RNA polymerase-promotor search. For all these examples, the reaction process represents finding a specific target on DNA by a combination of 3D and 1D diffusion. Our approach is sufficiently versatile to extend the proposed model to the case of a reversible reaction or immobility of one of the reactants on a 1D sink, which makes it especially relevant for systems where search on DNA plays an important role.

We believe that the proposed model represents a valuable tool in describing not only biologically relevant 1D search problems, but will also help in the development of synthetic and biomimetic approaches that aim for reaction optimization by reduction of search dimensionality.

ACKNOWLEDGMENTS

We would like to acknowledge funding from the Netherlands Organization for Scientific Research (NWO, Vici 680-47-607) and the European Research Council (ERC Starting Grant 281098).

APPENDIX: BIMOLECULAR REACTION IN SOLUTION WITH SHORT *D* SINKS

The D sink is considered to be short if $L_D < \sqrt{D_{AL}\tau_A}$, $\sqrt{D_{BL}\tau_B}$, and $L_D \sim 2r_{A,B}$. To distinguish between long D sinks (long DNA chains) and short D sinks (DNA fragments) the latter will be called molecules F. As distinct from the model of previous sections we do not introduce linear concentrations $n_{A,B,C}$. Instead, we assume that at a given time moment only one molecule A, B, or C can be trapped by F molecule. Migration of trapped molecules along the F molecule is neglected. Consider reactions between A, B, and F molecules in a buffer solution. All species are assumed to be mobile. F molecules can transiently trap molecules A and B to form complexes F-A and F-B, which will be denoted as Fa and Fb, respectively. The reactions between all species are listed below:

$$A + B \to C \quad \text{stable reaction product: molecule } C, \tag{A1}$$

$$A + F \leftrightarrow Fa \quad \text{complex } F\text{-}A \text{ with lifetime } \tau_A, \tag{A2}$$

$$B + F \leftrightarrow Fb \quad \text{complex } F\text{-}B \text{ with lifetime } \tau_B, \tag{A3}$$

$$C + F \leftrightarrow Fc \quad \text{complex } F\text{-}C \text{ with lifetime } \tau_C, \tag{A4}$$

$$A + Fb \to Fc \quad \text{molecule } C \text{ trapped on molecule } F, \tag{A5}$$

$$B + Fa \to Fc \quad \text{molecule } C \text{ trapped on molecule } F. \tag{A6}$$

The reaction between complexes Fa and Fb has low probability, e.g., because of high negative charge of DNA. The rate coefficients for reaction of A, B, and C with F, Fa, and Fb are constructed using capture efficiency (19):

$$\alpha_{iF} = Z_i L_F (D_i + D_F), \quad i = A,B,C, \tag{A7}$$

$$\alpha_{AFb} = \beta Z_A L_F (D_A + D_{Fb}), \tag{A8}$$

$$\alpha_{BFa} = \beta Z_B L_F (D_B + D_{Fa}), \tag{A9}$$

where L_F is the length of F molecules and $D_{F,Fa,Fb}$ are diffusion coefficients approximated by the Stokes-Einstein equation for a sphere of the same volume,

$$D_F = \frac{k_B T}{6\pi\mu}\left(\frac{3}{4} r_D^2 L_F\right)^{-1/3}, \tag{A10}$$

$$D_{Fa,Fb} = \frac{k_B T}{6\pi\mu}\left(\frac{3}{4} r_D^2 L_F + r_{A,B}^3\right)^{-1/3}. \tag{A11}$$

The mean concentrations of molecules and complexes obey the rate equations corresponding to reactions (A1)–(A6):

$$\frac{dC_A}{dt} = -\alpha_{AB} C_A C_B - \alpha_{AF} C_A C_F - \alpha_{AFb} C_A C_{Fb} + \frac{C_{Fa}}{\tau_A}, \tag{A12}$$

$$\frac{dC_B}{dt} = -\alpha_{AB} C_A C_B - \alpha_{BF} C_B C_F - \alpha_{BFa} C_B C_{Fa} + \frac{C_{Fb}}{\tau_B}, \tag{A13}$$

$$\frac{dC_F}{dt} = -\alpha_{AF} C_A C_F - \alpha_{BF} C_B C_F - \alpha_{CF} C_C C_F + \frac{C_{Fa}}{\tau_A} + \frac{C_{Fb}}{\tau_B} + \frac{C_{Fc}}{\tau_C}, \tag{A14}$$

$$\frac{dC_{Fa}}{dt} = -\alpha_{AF} C_A C_F - \alpha_{BFa} C_B C_{Fa} - \frac{C_{Fa}}{\tau_A}, \tag{A15}$$

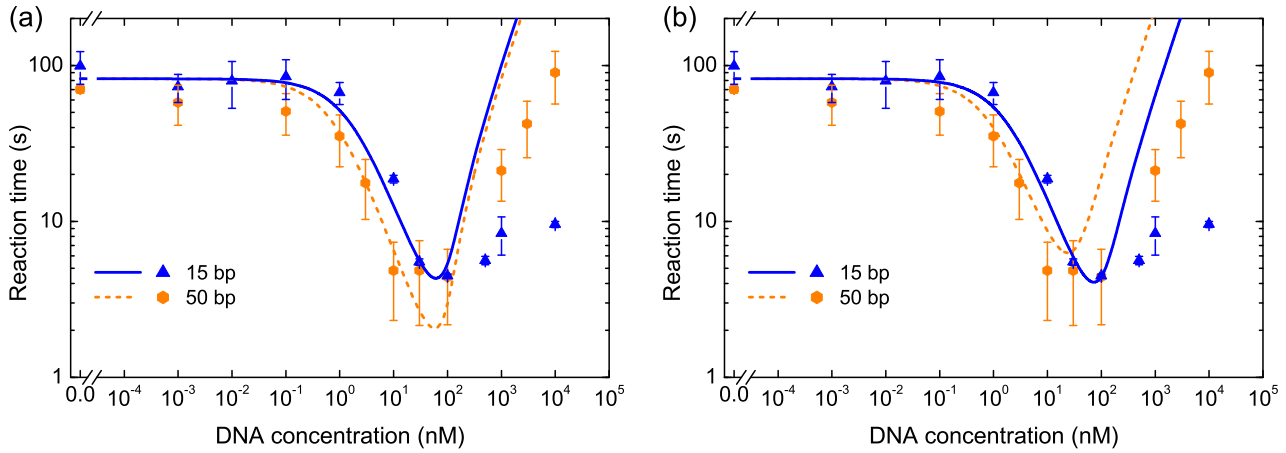

FIG. 10. (Color online) Dependence of the reaction time on the concentration of short DNA fragments. Comparison of the experimental data (symbols) to the predictions of the models (lines). (a) Calculations with Eqs. (A12)–(A20) for short D sinks. (b) Calculations with the model of Sec. II for long D sinks; here 1D diffusion coefficients $D_{AL} = D_{BL}$ and $D_D \neq 0$ [see Eq. (57)].

$$\frac{dC_{Fb}}{dt} = -\alpha_{BF}C_BC_F - \alpha_{AFb}C_AC_{Fb} - \frac{C_{Fb}}{\tau_B}, \tag{A16}$$

$$\frac{dC_{Fc}}{dt} = \alpha_{AFb}C_AC_{Fb} + \alpha_{BFa}C_BC_{Fa} + \alpha_{CF}C_CC_F - \frac{C_{Fc}}{\tau_C}, \tag{A17}$$

$$\frac{dC_C}{dt} = \alpha_{AB}C_AC_B - \alpha_{CF}C_CC_F + \frac{C_{Fc}}{\tau_C}. \tag{A18}$$

The overbar denoting mean values is omitted here [cf. Eqs. (38)–(43)]. The initial conditions are

$$C_A|_{t=0} = C_{A0}, \quad C_B|_{t=0} = C_{B0}, \quad C_F|_{t=0} = C_{F0}, \tag{A19}$$

$$C_{Fa}|_{t=0} = C_{Fb}|_{t=0} = C_{Fc}|_{t=0} = C_C|_{t=0} = 0. \tag{A20}$$

Let us derive the conditions under which molecules F accelerate the reaction between A and B molecules. The total concentration of the reaction product $C_C^T = C_C + C_{Fc}$ changes with time according to the equation

$$\frac{dC_C^T}{dt} = \alpha_{AB}C_AC_B + \alpha_{AFb}C_AC_{Fb} + \alpha_{BFa}C_BC_{Fa}, \tag{A21}$$

which can be rewritten in terms of total concentrations of A and B molecules $C_{A,B}^T = C_{A,B} + C_{Fa,Fb}$,

$$\frac{dC_C^T}{dt} = \alpha_{AB}C_A^TC_B^T + \alpha_{AB}\Delta R, \tag{A22}$$

where the first term on the right side is the reaction rate in solution without molecules F, while ΔR is the contribution to the reaction rate due to F molecules,

$$\Delta R = C_{Fa}C_{Fb}\left[\left(\frac{\alpha_{AFa}}{\alpha_{AB}} - 1\right)\frac{C_A}{C_{Fa}} + \left(\frac{\alpha_{BFa}}{\alpha_{AB}} - 1\right)\frac{C_B}{C_{Fb}} - 1\right]. \tag{A23}$$

It is seen that $\Delta R < 0$ if the term in square brackets is negative, e.g., at $\alpha_{AFa}/\alpha_{AB} < 1$ and $\alpha_{BFa}/\alpha_{AB} < 1$. In this case the addition of molecules F to the solution would retard the reaction between A and B molecules. The catalytic effect of molecules F is observed when $\Delta R > 0$, e.g., at $\alpha_{AFa}/\alpha_{AB} > 1$ and $\alpha_{BFa}/\alpha_{AB} > 1$. Two latter conditions imply that, as compared to the reaction between free A and B molecules in solution, complexes Fa and Fb effectively attract free B and A molecules, thereby providing a place for the reaction between free and trapped A and B molecules.

Figure 10 compares model predictions with the experimental data for the DNA fragments of 5 nm (15 bp) and 16.7 nm (50 bp). It should be emphasized that in calculations we used the same set of reaction factors γ_{AB}, γ_D, and β as in the model for long D sinks. For the parameters chosen to calculate the reaction time the ratios

$$\frac{\alpha_{AFa}}{\alpha_{AB}} \approx \frac{\alpha_{BFb}}{\alpha_{AB}} \approx \begin{cases} 38 & \text{at } L_F = 5 \text{ nm} \\ 81 & \text{at } L_F = 17.5 \text{ nm} \end{cases}. \tag{A24}$$

It is seen that predictions of models for short [Fig. 10(a)] and long D sinks [Fig. 10(b)] qualitatively agree.

[1] G. Adam and M. Delbrück, *Structural Chemistry and Molecular Biology* (Freeman, San Francisco, 1968), pp. 198–215.

[2] A. D. Riggs, S. Bourgeois, and M. Cohn, J. Mol. Biol. **53**, 401 (1970).

[3] O. G. Berg and M. Ehrenberg, Biophys. Chem. **15**, 41 (1982).

[4] O. G. Berg, R. B. Winter, and P. H. von Hippel, Biochemistry **20**, 6929 (1981).

[5] R. B. Winter, O. G. Berg, and P. H. von Hippel, Biochemistry **20**, 6961 (1981).

[6] P. H. von Hippel and O. G. Berg, J. Biol. Chem. **264**, 675 (1989).

[7] S. E. Halford and J. F. Marko, Nucleic Acids Res. **32**, 3040 (2004).

[8] K. V. Klenin, H. Merlitz, J. Langowski, and C. X. Wu, Phys. Rev. Lett. **96**, 018104 (2006).

[9] S. E. Halford and M. D. Szczelkun, Eur. Biophys. J. **31**, 257 (2002).
[10] J. Gorman and E. C. Greene, Nat. Struct. Mol. Biol. **15**, 768 (2008).
[11] T. Hu, A. Y. Grosberg, and B. I. Shklovskii, Biophys. J. **90**, 2731 (2006).
[12] M. Slutsky and L. A. Mirny, Biophys. J. **87**, 4021 (2004).
[13] T. Hu and B. I. Shklovskii, Phys. Rev. E **74**, 021903 (2006).
[14] M. Barbi, C. Place, V. Popkov, and M. Salerno, Phys. Rev. E **70**, 041901 (2004).
[15] I. M. Sokolov, R. Metzler, K. Pant, and M. C. Williams, Phys. Rev. E **72**, 041102 (2005).
[16] H. Merlitz, K. V. Klenin, and J. Langowski, J. Chem. Phys. **124**, 134908 (2006).
[17] A.-M. Florescu and M. Joyeux, J. Chem. Phys. **130**, 015103 (2009).
[18] A.-M. Florescu and M. Joyeux, J. Chem. Phys. **131**, 105102 (2009).
[19] E. F. Koslover, M. A. Díaz de la Rosa, and A. J. Spakowitz, Biophys. J. **101**, 856 (2011).
[20] P. C. Blainey, V. Graziano, A. J. Péres-Berná, W. J. McGrath, S. Jane Flint, C. San Martín, X. Sunney Xie, and W. F. Mangel, J. Biol. Chem. **288**, 2092 (2013).
[21] V. Graziano, G. Luo, P. C. Blainey, A. J. Péres-Berná, W. J. McGrath, S. Jane Flint, C. San Martín, X. Sunney Xie, and W. F. Mangel, J. Biol. Chem. **288**, 2068 (2013).
[22] A. Turkin, L. Zhang, A. Marcozzi, W. F. Mangel, A. Herrmann, and A. M. van Oijen, Chem. Sci. (2015), doi:10.1039/C5SC03063C.
[23] S. L. Hardt, Biophys. Chem. **10**, 239 (1979).
[24] L. W. Anacker and R. Kopelman, J. Chem. Phys. **81**, 6402 (1984).
[25] A. Molski and J. Keizer, J. Chem. Phys. **94**, 574 (1991).
[26] A. Molski, Chem. Phys. Lett. **178**, 43 (1991).
[27] Z. Rácz, Phys. Rev. Lett. **55**, 1707 (1985).
[28] Z.-Y. Shi and R. Kopelman, Chem. Phys. **167**, 149 (1992).
[29] L. W. Anacker, R. P. Parson, and R. Kopelman, J. Phys. Chem. **89**, 4758 (1985).
[30] A. D. Brailsford and R. Bullough, Philos. Trans. R. Soc., A **302**, 87 (1981).
[31] G. S. Was, *Fundamentals of Radiation Materials Science: Metals and Alloys* (Springer, Berlin, 2007).
[32] P. Debye, Trans. Electrochem. Soc. **82**, 265 (1942).
[33] M. Smoluchowski, Z. Phys. Chem. **92**, 129 (1917).
[34] D. Shoup, G. Lipari, and A. Szabo, Biophys. J. **36**, 697 (1981).
[35] O. G. Berg and P. H. von Hippel, Ann. Rev. Biophys. Biophys. Chem. **14**, 131 (1985).
[36] O. G. Berg, Biophys. J. **47**, 1 (1985).
[37] F. C. Collins and G. E. Kimball, J. Colloid Sci. **4**, 425 (1949).
[38] N. Agmon and A. Szabo, J. Chem. Phys. **92**, 5270 (1990).
[39] G. Schreiber, G. Haran, and H.-X. Zhou, Chem. Rev. **109**, 839 (2009).
[40] A. V. Barzykin and A. I. Shushin, Biophys. J. **80**, 2062 (2001).
[41] A. I. Shushin and A. V. Barzykin, Biophys. J. **81**, 3137 (2001).
[42] H.-X. Zhou, Q. Rev. Biophys. **43**, 219 (2010).
[43] P. H. Richter and M. Eigen, Biophys. Chem. **2**, 255 (1974).
[44] R. Schranner and P. H. Richter, Biophys. Chem. **8**, 135 (1978).
[45] T. R. Waite, Phys. Rev. **107**, 463 (1957).
[46] H. S. Carslaw and J. C. Jaeger, *Conduction of Heat in Solids* (Clarendon Press, Oxford, 1959).
[47] R. Bullough, M. R. Hayns, and M. H. Wood, J. Nucl. Mater. **90**, 44 (1980).
[48] A. Suna, Phys. Rev. B **1**, 1716 (1970).
[49] E. Hairer and G. Wanner, *Solving Ordinary Differential Equations II. Stiff and Differential-Algebraic Problems* (Springer-Verlag, Berlin, 1996).
[50] G. Akerlof, J. Am. Chem. Soc. **54**, 4125 (1932).
[51] Y. M. Wang, R. H. Austin, and E. C. Cox, Phys. Rev. Lett. **97**, 048302 (2006).
[52] J. Elf, G. W. Li, and X. S. Xie, Science **316**, 1191 (2007).
[53] A. Tafvizi, F. Huang, A. R. Fersht, L. A. Mirny, and A. M. van Oijen, Proc. Natl. Acad. Sci. USA **108**, 563 (2011).
[54] A. G. Cherstvy, A. B. Kolomeisky, and A. A. Kornyshev, J. Phys. Chem. B **112**, 4741 (2008).